Applied Thermal Engineering 41 (2012) 84–91

Contents lists available at SciVerse ScienceDirect

Applied Thermal Engineering

journal homepage: www.elsevier.com/locate/apthermeng

Performance tests of two small trigeneration pilot plants

M.S. Rocha [a], R. Andreos [b], J.R. Simões-Moreira [b,c,*]

[a] IPEN/CNEN – Nuclear and Energy Research Institute, Av. Lineu Prestes 2242, São Paulo 05508-000, SP, Brazil
[b] IEE – Institute of Electrotechnical and Energy, University of São Paulo, Av. Prof. Luciano Gualberto 1289, São Paulo 05508-010, SP, Brazil
[c] SISEA – Alternative Energy Systems Laboratory, Department of Mechanical Engineering, Escola Politécnica, University of São Paulo, Av. Prof. Mello Moraes 2231, São Paulo 05508-900, SP, Brazil

A R T I C L E   I N F O

Article history:
Received 11 April 2011
Accepted 5 December 2011
Available online 11 December 2011

Keywords:
Cogeneration
Trigeneration
CCHP

A B S T R A C T

Trigeneration systems have been used with advantage in the last years in distributed electricity generation systems as a function of a growth of natural gas pipeline network distribution system, tax incentives, and energy regulation policies. Typically, a trigeneration system is used to produce electrical power simultaneously with supplying heating and cooling load by recovering the combustion products thermal power content that otherwise would be driven to atmosphere. Concerning that, two small scale trigeneration plants have been tested for overall efficiency evaluation and operational comparison. The first system is based on a 30 kW (ISO) natural gas powered microturbine, and the second one uses a 26 kW natural gas powered internal combustion engine coupled to an electrical generator as a prime mover. The stack gases from both machines were directed to a 17.6 kW ammonia–water absorption refrigeration chiller for producing chilled water first and next to a water heat recovery boiler in order to produce hot water. Experimental results are presented along with relevant system operational parameters for appropriate operation including natural gas consumption, net electrical and thermal power production, i.e., hot and cold water production rates, primary energy saving index, and the energy utilization factor over total and partial electrical load operational conditions.

1. Introduction

Energy concern has been considered as an important variable for governmental police makers lately as well as for commercial and industrial production cost reduction. It has been drawn an energy shortage scenario for the near future, which boosts new technologies and processes development aiming at a continuous efficiency growth in using a given primary energy source. In this way, distributed energy systems have been largely investigated as an economical way for supplying electrical and thermal energy, mainly for special applications in which reliability is a key point [1–3]. Attention has increasingly been driven to an efficiently and environmentally sustainable useful electrical and thermal power production. Combined cooling, heat, and power (CCHP) or trigeneration systems is a relatively old technology that converts the energy content in the fuel chemical bonds into a simultaneous production of electricity, heating, and cooling. It has become an economical available machinery configuration to supply those demands from a single source of primary energy, with the advantages of saving energy, money, and making an environmental intelligent use of fossil fuels [4,5]. By generating electricity on site, the typical losses associated with transmission of electricity basically vanish. Also, the thermal energy in stack gases can be used for on-site production of either heating, or cooling, or both, as in our case.

Presently, distributed energy systems represent less than 10% of total energy produced worldwide [6]. A trigeneration system has the great potential of reducing carbon emission and air pollutant emissions besides it can increase energy efficiency of power plants [7,8], hotels [9], hospitals [10], supermarkets [11–13], airports [14], and shopping centers [15]. The potential of energy savings by using the CCHP systems in many countries have increased in the last years as a function of natural gas infrastructure network distribution growth in populated urban centers, fuel tax incentive as well as energy regulations by federal governments concerning distributed electrical power generation in those countries.

Concerning fossil fuels used for electrical power generation, natural gas is the one more environmentally friend than other fossil fuels due to its low rates of gaseous or none pollutant emissions and it also presents a clean burning process. Micro cogeneration systems offer greater overall energy efficiency than conventional

* Corresponding author. IEE – Institute of Electrotechnical and Energy, University of São Paulo, Av. Prof. Luciano Gualberto 1289, São Paulo 05508-010, SP, Brazil. Tel.: +55 11 30915684; fax: +55 11 38131886
E-mail address: jrsimoes@usp.br (J.R. Simões-Moreira).

1359-4311/$ – see front matter © 2011 Elsevier Ltd. All rights reserved.
doi:10.1016/j.applthermaleng.2011.12.007

electricity generation by central thermal power plants, achieving less primary energy consumption, reducing CO_2 emissions and lowering energy costs [16].

Trigeneration systems can be characterized by electrical power generation of a few kilowatts to dozens of megawatts; they are also located near to final users, avoiding expensive transmission lines that accounts for considerable losses. Typical efficiency of a central power plant (combined cycle configuration) can reach at most 55%, a micro CCHP technology can achieve efficiencies up to 85% [6], considering all forms of useful energy produced. Heat is recovered from the prime energy engine stack gases by a heat recovery system, and chilled water is obtained by incorporating an absorption refrigeration chiller that is also powered by the waste heat from the hot stack gases [17–19]. The introduction of an absorption chiller in a trigeneration system implies in increasing the overall efficiency of the fuel molecule energy content. In a recent work, Preter et al. [20] published experimental results of a trigeneration system in which cooling water was produced from recovering waste heat of a 30 kW_{el} (ISO conditions) microturbine using an adapted direct fire absorption chiller, showing that, for some specific operational condition it is possible to obtain relatively overall system primary energy utilization factor as high as 70%.

Two configurations of trigeneration systems have been tested by the authors. The first one is based in a natural gas fired microturbine as the prime mover and a commercial ammonia–water based absorption cycle for chilled water production, and a heat recovery boiler for hot water production. The second trigeneration system tested is based in a natural gas fired internal combustion engine with the two other waste heat recovery systems just mentioned. In this paper it is presented the experimental aspects of operation of those systems. A comparative evaluation of two design options of trigeneration systems was carried out as a method of establishing a decision planning strategy before the selection of the actual most convenient alternative for a given application. The comparison was carried out by performing mainly technical analyses aspect of trigeneration systems.

2. Trigeneration system description

The CCHP developed and tested in the laboratory was composed of two different system configurations: a system using a microturbine (MT), and a system using an internal combustion engine (ICE). In both cases the combustion products were driven to an absorption refrigeration chiller (ARC) and to a heat recovery boiler (HRB). The absorption chiller used was originally a direct fired natural gas powered commercial model, and it was technically modified in order to operate with the stack gases. Some modifications into its electronic control system were performed too. Equipment specifications are given in Table 1. Previous authors [21,22] have tested similar systems separately.

The coefficient of performance (*COP*) of a commercial ammonia–water single stage absorption chiller varies between 0.6 and 0.7, depending on the condensing and evaporating temperatures. Originally, the direct fired ARC had a built-in flute type burner. The combustion chamber and the heating system were modified by replacing the flute type burner by a new device built to receive the hot stack gases from either the MT or the ICE. Additionally, the chiller ignition system originally designed to control the flute type burner was replaced by a manual driver system.

Fig. 1a shows the schematics of the first trigeneration system configuration formed by the microturbine, the heat recovery boiler, and the ammonia–water absorption chiller. Fig. 1a also shows additional and supporting subsystems for the trigeneration test rig which are: a natural gas compressor (GC); a cooling load

Table 1
The two trigeneration system equipment description and operational data.

Equipment	Model/manufacture	Characteristics
Microturbine (MT)	Capstone C30 [23]	Power = 30 kW_{el} (ISO), 400 V/3 phase Natural Gas[a]
Internal Combustion Engine (ICE)	Leon Heimer ATED 19/21 [24]	Power = 33 kVA, 220 V/3 phase Natural Gas[b]
Gas Compressor (GC)	CompAir V04G [25]	P_{max} = 6.5 bar Q_{max} = 36 m^3/h
Heat Recovery Boiler (HRB)	Unifin Micogen MG1-C1 [26]	Max Heat Recovery = up to 73 kW_{th}
Ammonia–Water Absorption Chiller(ARC)	Robur GAHP-AR [27]	Cooling Capacity = 17 kW_{th} Natural Gas

[a] Data from Capstone Microturbine Corporation.
[b] Data from Leon Heimer S/A.

circuit for simulating the air conditioning load (Q_{ARC}); a heating load circuit that simulated the hot water load (Q_{HW}); an electrical transformer to connect the MT to the building power grid. As seen in Fig. 1, the combustion products are driven to both the ARC and the HRB. Dumpers D_1 and D_2 allow controlling the mass flow rate to each piece of equipment. Fig. 1b shows a still picture of the three main components assembled together for operation and tests.

The second system configuration was similar to the first one, except for the fact that the MT was replaced by the internal combustion engine as can be seen in schematics in Fig. 2a. A still picture of this second trigeneration system is shown in Fig. 2b. In this second configuration two other modifications were necessary: the natural gas compressor for the ICE was unnecessary because the ICE ran at a low pressure natural gas (3.0 kPa); the ICE's switchboard load transfer panel (Fig. 2a) could not make load parallelism to the local power grid in opposition to the MT, so a resistive electrical load simulator system composed by three different electrical load levels (9.0, 18.0, and 21.0 kW) was built to dissipate the electricity produced by the electrical generator, as one can see in the schematics in Fig. 2a.

Temperature measurements of combustion gases, natural gas, hot water, cold water, and admission air were made with *K* and *T* type thermocouples with nominal uncertainty level of ± 0.1 °C. Natural gas flow was measured with a natural gas volumetric metering type with uncertainty of ± 0.0001 m^3/h. Combustion gases pressure and velocity were measured in two points by taking the gas velocities using a 3 mm O.D. and 100 mm long Pitot tube. Combustion gases flow was calculated by the EPA Methods [28–30] with calculated uncertainty of ± 0.05 kg/s. Hot and cold water flows were measured using specific volumetric metering types with uncertainties of ± 0.001 m^3/h. Electrical power was measured using a multiple parameters digital transducer. The experimental data were stored using a PC and a data acquisition system NI DAQ-9172 was used.

Electricity tracking operation mode was established for the trigeneration system. Firstly, the system had to supply the electrical energy to meet the electrical energy demand; next the thermal energy from the combustion gases was driven for producing chilled water in ARC; and, finally, the remaining thermal energy from the hot flue gases was recovered for water heating. It is important to stress that the major part of the stack gases from either the MT or the ICE was driven to the ammonia–water absorption cycle (ARC) for production of chilled water.

Thermal load (Q_{AC}) was applied to the chilled water circuit to simulate an actual situation, such as a commercial installation, where chilled water should be used for air conditioning system. The

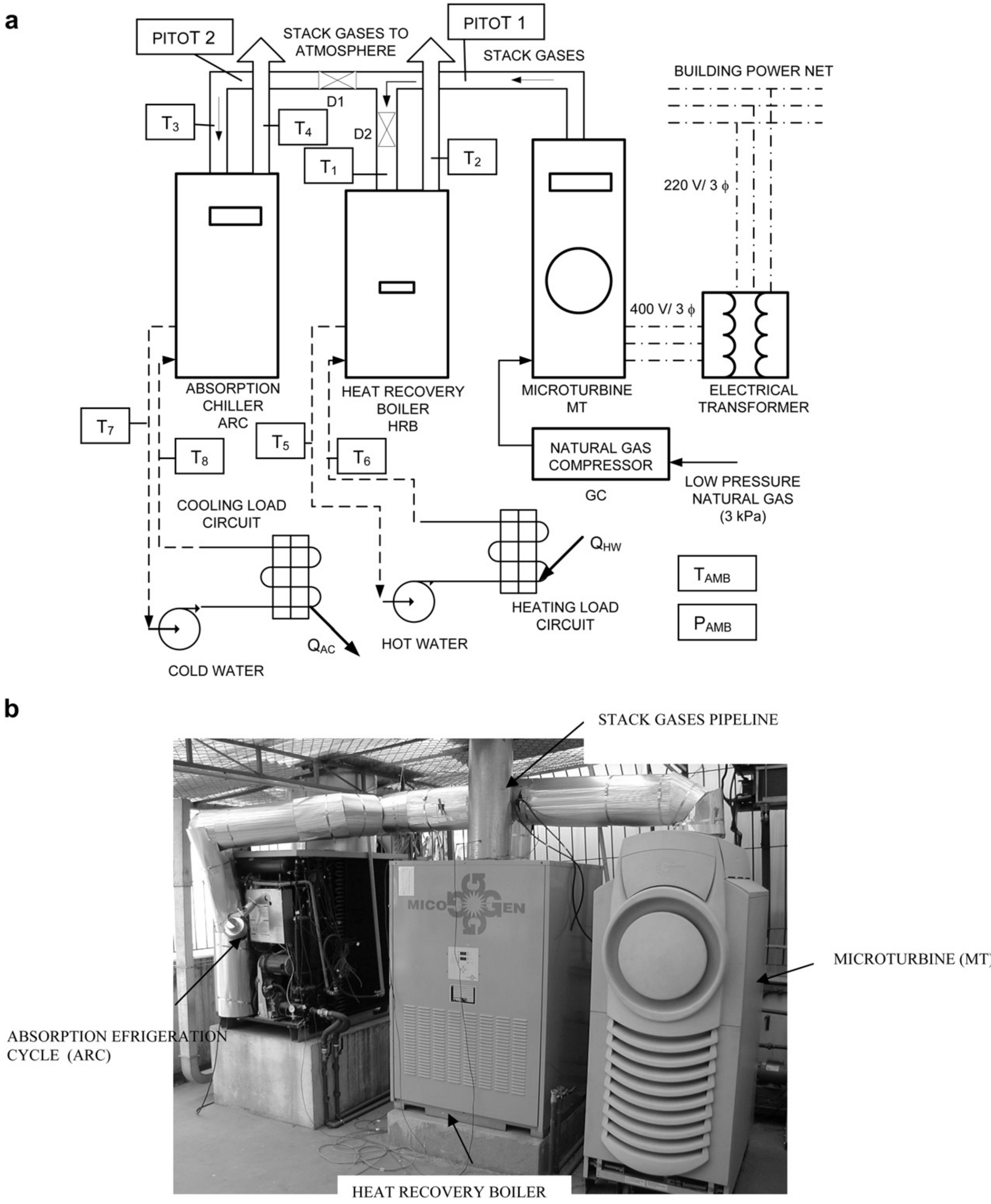

Fig. 1. Trigeneration system with MT. (a) schematics showing the machinery and supporting testing equipment; (b) still picture of the assembled system.

remaining thermal energy of stack gases was recovered by the heat recovery boiler unit (HRB) to produce hot water. A thermal load simulation system (Q_{HW}) for the hot water was also built to simulate an actual installation.

The cogeneration plant efficiency is, normally, measured by evaluation indexes used to establish a global system performance. In this work, two indexes were used: the first is the Energy Utilization Factor, or *EUF*, proposed in [31], which is defined as follows in Eq. (1):

$$EUF = \frac{(EP_{TS}) + (Q_{HRB} + Q_{ARC})}{FP} \tag{1}$$

where, EP_{TS} is the electrical power produced by microturbine or internal combustion engine, Q_{HRB} is the useful heating power

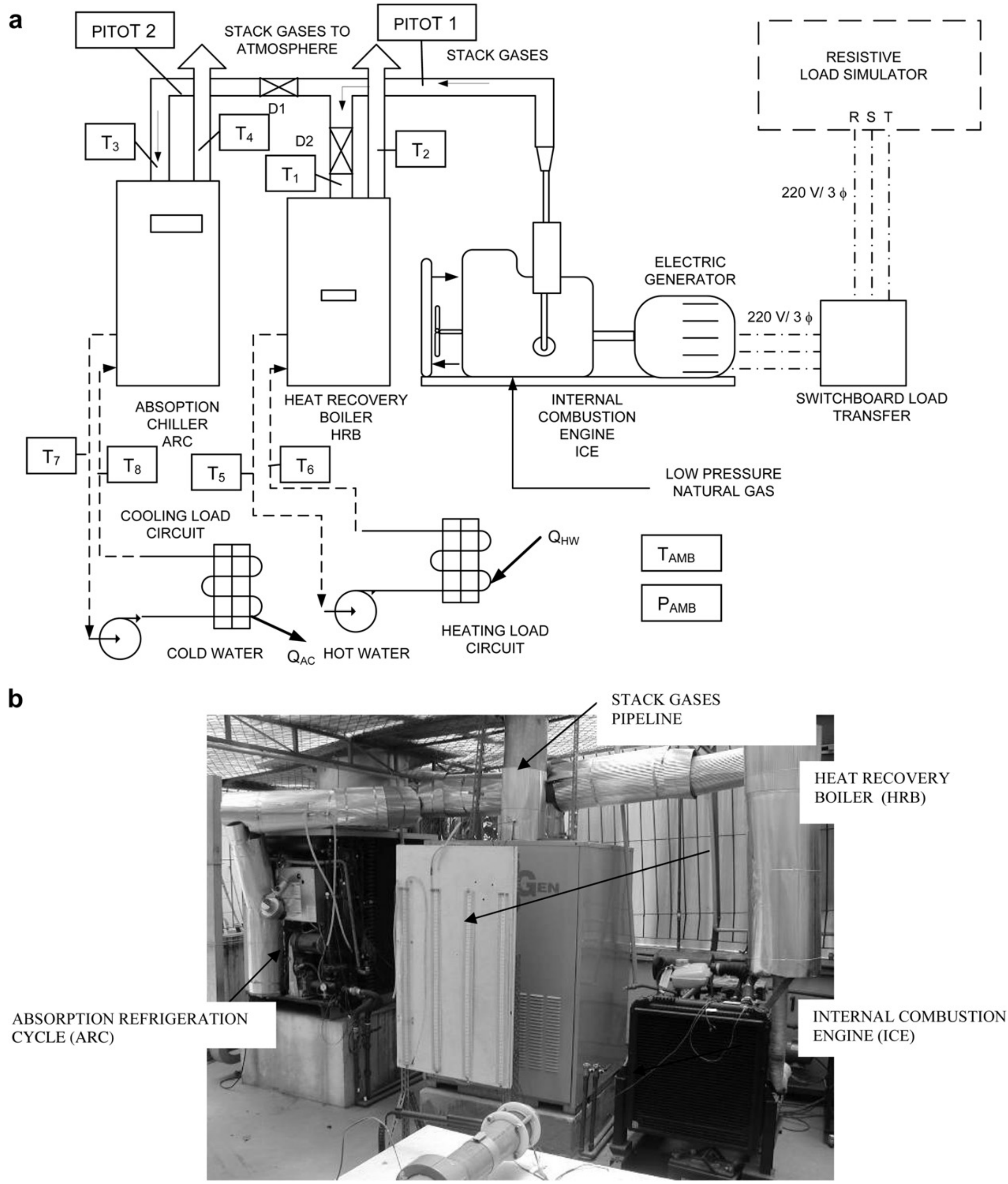

Fig. 2. Trigeneration system with ICE. (a) schematics showing the machinery and supporting testing equipment; (b) still picture of the assembled system.

produced by heat recovery boiler, Q_{ARC} is the useful cooling load produced by absorption chiller, and FP is the total available heating power obtained from burning fuel. FP, is calculated according to Eq. (2):

$$FP = m_F \times LHV \tag{2}$$

where, m_F is the measured fuel mass flow rate and LHV is the fuel lower heating value. A slight modification in Eq. (1) was introduced in order to take away the self-electricity consumption accounted by EC_{TS}.

Using the EUF concept and accounting the total electrical power consumed by the trigeneration system (EC_{TS}), Eq. (1) becomes:

$$EUF = \frac{(EP_{TS} - EC_{TS}) + (Q_{HRB} + Q_{ARC})}{FP} \tag{3}$$

The second performance index is the PES (Primary Energy Saving), as described in [32], established by the European Directive, which is a methodology for determining the efficiency of cogeneration systems given by the Primary Energy Saving, PES, given by Eq. (4):

$$PES = \left(1 - \frac{1}{\frac{CHP\ H_\eta}{Ref\ H_\eta} + \frac{CHP\ E_\eta}{Ref\ E_\eta}}\right) \tag{4}$$

where, $CHP\ H_\eta$ and $CHP\ E_\eta$ are, respectively, the average thermal and electrical efficiency of a CHP plant or process during an operation year, and $Ref\ H_\eta$ and $Ref\ E_\eta$ are, respectively, the reference efficiencies of separate thermal and electric production processes. According to other authors [32,33], a CCHP plant must present a *PES* as high as 10% to be considered as an efficient one. All of those magnitudes were either directly measured or calculated for both tested systems. According to [33], the reference efficiency of thermal production processes $Ref\ H_\eta = 0.9$, and the reference efficiency of electric production processes $Ref\ E_\eta = 0.525$. Table 2 presents the values used to perform the trigeneration systems *EUF* and *PES* calculation in next section.

3. Results and analysis

3.1. Trigeneration operating with microturbine

Table 2 shows the experimental data for the inlet and outlet temperatures, inlet and outlet flow rates of gases and water of each piece of equipment of the first trigeneration system based on the microturbine as the prime mover. During all tests, the ammonia–water absorption chiller was setup for the maximum specified cooling capacity 17.6 kW_{th} at a condensing temperature of 30 °C and a cooling water delivery temperature at 7 °C with a temperature difference of 10 °C (difference between chilled water delivered and returned). The average volumetric water flow rate measured was 2.0 m^3/h. The heat recovery boiler was setup for gas temperature limits between 260 °C and 370 °C, and hot water temperature limits of 20 °C–80 °C. The volumetric hot water average flow rate was 1.86 m^3/h.

Two test runs were carried out with the microturbine: one for partial power set at 15 kW_{el} (50% of electrical ISO power capacity), and the other for the maximum local electrical power delivered by the microturbine at site condition, which, achieved 24 kW_{el}. It is important to note that the measured average electrical power consumed by the trigeneration system EC_{TS} was 1.5 kW_{el}.

Results from temperature and mass flow rates measurements are presented for the local condition as shown in Table 2. During the tests, the average on site conditions were: atmospheric pressure, $P_{atm} = 93.3$ kPa; environmental average temperature of 20 °C; and relative humidity of 66%. ISO conditions are: environmental temperature of 15 °C, relative humidity of 60%, and ambient pressure of 101.325 kPa.

All tests were carried out with the dump valve *D*1 (refer to Fig. 1a) fully opened (100%) and the dump valve *D*2 partially opened (50%), which permitted a higher flow of stack gases to be directed to the absorption chiller, and less hot gases flow reached the heat recovery system. This operational condition was imposed to guarantee that the full absorption chiller cooling capacity was obtained.

When the microturbine ran at 15 kW_{el}, the total stack gases mass flow rate measured was 0.186 kg/s, the available thermal power in the stack gases was about 53.2 kW_{th}, and the heat rate was 4.4. When the microturbine was producing 24 kW_{el} (maximum power), the stack gases mass flow rate was 0.289 kg/s, the available thermal power in the stack gases was 96.8 kW_{th}, and the heat rate was 3.9 as can be seen in Table 2. The stack gases thermal power E_{EG} is defined as follows:

$$E_{SG} = m_{SG} C_{p-SG} (T_{SG} - T_{amb}) \tag{5}$$

where, m_{SG} is the stack gases mass flow rate, C_{p-SG} is the stack gases average specific heat at constant pressure, T_{SG} and T_{amb} are the stack gases and environment air temperatures, respectively. A precise stack gas analysis would require knowing its chemical composition. However, it was considered the stack gases average specific heat as the nitrogen's, i.e., $C_{p-SG} = C_{p-N2} = 1.04$ kJ/kg K [34].

The heat rate, *HR*, is the ratio between the total available fuel power, *FP*, to the net electrical power, *EP*, is given by Eq. (6):

$$HR = \frac{FP}{EP} \tag{6}$$

At the maximum cooling capacity of the absorption chilled an average $COP = 0.612$ was obtained [35], and, therefore, the minimum stack gas energy necessary to supply that cooling capacity was about 28 kW_{th}. From this simple energy analysis, the thermal power of the stack gases far exceeded the necessary thermal power to operate the absorption chiller at the maximum capacity, but this plain operational condition was not achieved in laboratory. Only on the second operational condition at a full electrical load (24 kW_{el}), the amount of thermal power available in the stack gases delivered by the microturbine (96.8 kW_{th}) was enough to produce the full chilled water load by the absorption chiller. After analyzing the chiller distillation column, where the thermal energy from the combustion gases is supplied to the chiller, it was noticed that it has a low effectiveness when operating under predominantly convective heat transfer regime as in the present case. Quite possibly, such a piece of equipment was initially designed and manufactured to operate predominantly by a combination of radiation and convective heat transfer modes as a consequence of direct fuel burning. So, the modifications completed in the absorption chiller generator revealed that the maximum cooling thermal power can be obtained only for the microturbine operating at maximum capacity.

The temperature difference (ΔT) was measured for both situations of partial and full electrical load over the ARC and HRB devices (Table 2). Stack gases mass flow rates were also measured and they are shown in that table. One can observe that the absorption chiller full operation can be attended just when the microturbine operates at 24 kW_{el}. In this way it is possible to determine the limit of operational condition of the trigeneration system designed to produce electrical energy as the primary demand to be met, chilled water (at 10 °C) and hot water (at 40 °C). For those results, and using Eq. (3), the *EUF* reached a 56.3% value. The *PES* calculated by

Table 2
Main measured data for the trigeneration systems based on the microturbine (MT) and on the internal combustion engine (ICE). $T_{air} = 20$ °C; $P_{atm} = 93.3$ kPa.

System parameters	MT		ICE	
	15 kW_{el}	24 kW_{el}	18 kW_{el}	21 kW_{el}
Natural gas flow rate, Q_{NG} (Nm^3/h)	7.3	10.5	8.8	9.6
Total stack gas mass flow rate, m_{SG} (kg/s)	0.186	0.289	0.026	0.032
Stack gas temperature from prime mover (°C)	295	342	500	586
Differential gas temperature in HRB (°C)	57.2	26.3	383	392
Differential gas temperature in ARC (°C)	86.1	138.8	248	264
Electrical efficiency (%)	22.6	25.6	25.8	27.6
Total stack gas thermal power, E_{SG} (kW_{th})	53.2	96.8	13.0	18.8
Heat Rate, *HR* (kW_{th}/kW_{el})	4.4	3.9	3.9	3.6
CHP Eη (%)		0.256		0.276
CHP Hη (%)		0.343		0.151
Ref Eη (%)		0.525		0.525
Ref Hη (%)		0.9		0.9

Eq. (4) reached 15.1%. Fig. 3 shows the energy flux diagram for the trigeneration system with MT. Data are for the full load operational mode as displayed in Table 2. As seen, due to the low effectiveness of the used ARC and in HRB in using the available thermal power from the stack gases, considerable thermal power still exits the trigeneration system with the combustion gases exhausted to atmosphere. This is a fact that draws attention to the effect that the heat recovery equipment in a trigeneration system must be sized to ensure the greatest efficiency possible. Accounted losses in this case were about 43.7%, as can be seen in Fig. 3.

3.2. *Trigeneration operating with internal combustion engine*

The second test battery was carried out having the ICE as the prime mover, as discussed in Section 2 (Fig. 2). Table 2 shows the main data obtained. The same setup parameters and local conditions from the first battery test occurred for these tests.

In this case, two test batteries were carried out with the ICE: one for electrical power setup at 18 kW_{el} (partial load), and the other for the full electrical power delivered by ICE, that in this case was 21 kW_{el}.

Tests were carried out having the damper *D*1 (see Fig. 2a) fully opened (100%) and the damper *D*2 partially opened (50%), which permitted a higher stack gases flow to be directed to the absorption chiller, and a small fraction of stack gases flowed to the heat recovery system. This operational condition was imposed to guarantee that the total absorption chiller cooling capacity was attended.

At partial electrical load (18 kW_{el}), the total stack gases thermal power delivered was 13 kW_{th}, which corresponded to a heat rate of 3.8, and in second case (21 kW_{el}), the total stack gases thermal power delivered was 18.8 kW_{th}, with a heat rate of 3.6. Temperatures of stack gases delivered by ICE reached the maximum temperature of 586 °C, according to the experimental results, and temperature difference at absorption chiller generator reached 392 °C. Therefore, at partial load (18 kW_{el}), from the total amount of thermal power capacity available in stack gases, E_{EG}, about 57% was effectively transformed into cooling load by absorption chiller ($COP = 0.57$, in this case). For the second case (21 kW_{el}), about 62% of total amount of thermal energy available in stack gases was effectively transformed into cooling load. It occurred because of low chiller generator efficiency due to the predominance of convective heat transfer phenomenon instead radiation heat transfer, as discussed above. The same could be observed for the microturbine case, although in that case, stack gases flow was much higher than for internal combustion engine's, enabling a higher use of thermal available energy. Using ICE as the prime mover, the *EUF* calculated by Eq. (3) reaches 42.7%, and the *PES* calculated by Eq. (4) reaches 44.2%.

It can be observed in Fig. 4 that the *EUF* reached 42.7% in the case of internal combustion engine (considering just stack gases as thermal power source). Changes in the heat recovery system configuration should be done to permit the use of a larger part of ICE available thermal power. It is noteworthy to mention that the engine water cooling jacket was not considered in this work and the cooling water energy was accounted as losses. Of course, there is a potential for using that thermal energy.

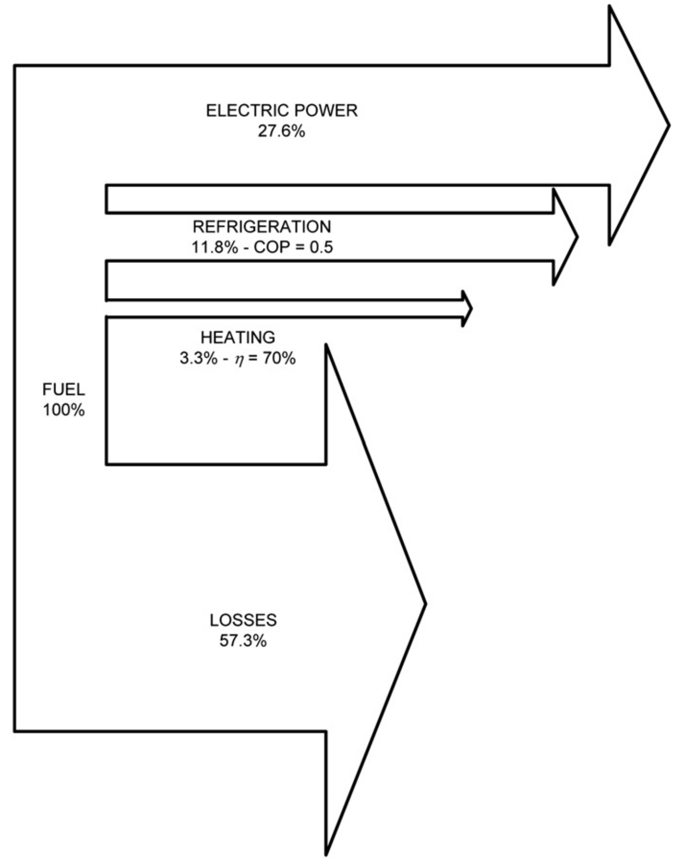

Fig. 4. Energy flux diagram for the trigeneration system operating with internal combustion engine, *EUF* = 42,7%, and *PES* = 44.2%. Magnitudes are calculated from data in Table 2.

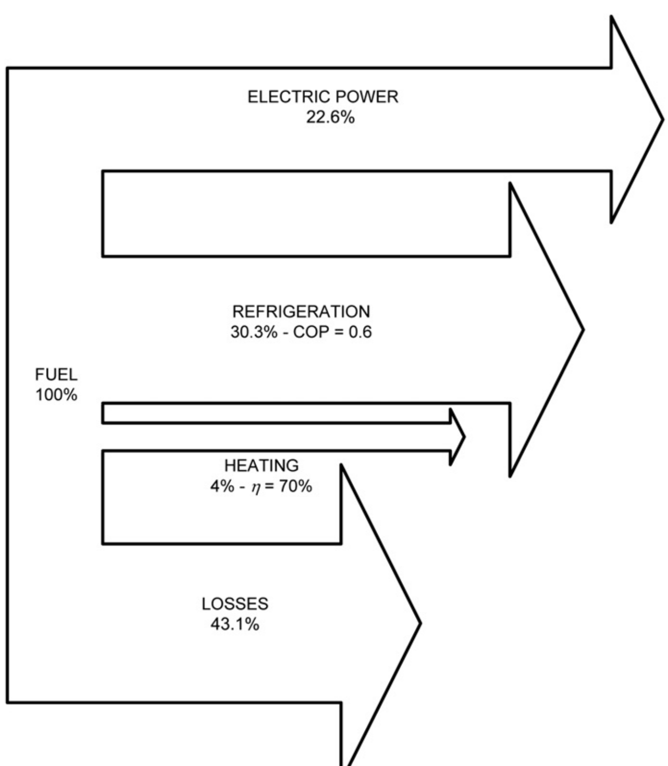

Fig. 3. Energy flux diagram for the trigeneration system operating with microturbine, *EUF* = 56.3%, and *PES* = 15.1%. Magnitudes are calculated from data in Table 2.

4. Conclusions

Experimental results were obtained for two trigeneration systems, one using microturbine, and other using an internal combustion engine as prime movers. Parameters for appropriate operation and system characterization including natural gas consumption, electrical power, hot and chilled water production over two operational conditions for the two trigeneration system configurations are presented. Results show that a *EUF* of 56.3%, and *PES* of 15.1% with a heat rate of 3.9 were obtained for the first configuration analyzed (MT). The second system configuration using ICE presented *EUF* of 43.7%, and *PES* of 44.2%, with a heat rate of 3.6. The thermal power from the engine water cooling jacket was not considered in this work and this thermal power can potentially be used as well. The heat recovery process in ARC and HRB (the compromise between stack gas temperature and mass flow rate) for both prime movers investigated is a key for the best small trigeneration plant efficiency.

Results show that both system configurations are viable, but modifications performed in absorption chiller (gases driven directly into the generator chamber) did not permit to obtain better *EUF*'s. It is suggested to carry out designing modifications in the ARC in order to improve the poor heat transfer process in the generator column, possibly using thermal fluids as the heat transfer fluid.

Acknowledgements

The authors wish to acknowledge COMGAS – Companhia de Gás de São Paulo (Brazil) for the project financial support. The second author also thanks CNPq for a research scholarship.

Nomenclature

ARC	absorption chiller
COP	coefficient of performance
C_p	specific heat at constant pressure [J/kg k]
EC_{TS}	total electrical power consumed by the trigeneration system, in Eq. (1) [W]
EP_{TS}	electrical power produced by trigeneration system (microturbine or internal combustion engine), in Eq. (1) [W]
EP_{TS}	total electrical power consumed by the trigeneration system, in Eqs. (1) and (2) [W]
EUF	energy utilization factor of trigeneration system, in Eq. (1)
FP	total available fuel power, in Eqs. (1), (2), and (6) [W]
HR	heat rate
HRB	heat recovery boiler
ICE	internal combustion engine
ISO	international organization for standardization (standard conditions specified in the following ratings: ambient temperature of 15 °C, relative humidity of 60%, and ambient pressure of 101.325 kPa).
LHV	lower heating value [J/kg]
MT	microturbine
m	mass flow rate [kg/s]
Q_{HRB}	useful heating power produced by heat recovery boiler, in Eqs. (1) and (2) [W]
Q_{ARC}	useful cooling power produced by absorption refrigeration chiller, in Eqs. (1) and (2) [W]

Subscripts

air	air
ARC	absorption refrigeration chiller
F	fuel
HRB	heat recovery boiler
ICE	internal combustion engine
el	electrical power
SG	stack gas
th	thermal power
TS	trigeneration system

Greek

η	Efficiency

References

[1] J.H. Horlock, Cogeneration–Combined Heat and Power: Thermodynamics and Economics, Krieger Publishing Company, Florida, 1997.
[2] T. Ackermann, G. Andersson, L. Söder, Distributed generation: a definition, Electric Power Systems Research 57 (2001) 195–204.
[3] G. Chicco, P. Mancarella, Distributed multi-generation: a comprehensive view, Renewable and Sustainable Energy Reviews 13 (2009) 535–551.
[4] D.W. Wu, R.Z. Wang, Combined cooling heating and power: a review, Progress in Energy and Combustion Science 32 (2006) 459–495.
[5] V. Kuhn, J. Kleneš, J. Bulatov, MicroCHP: overview of selected technologies, products and field tests results, Applied Thermal Engineering 28 (2008) 2039–2048.
[6] IEA–International Energy Agency Report, Combined Heat and Power – Evaluating the Benefits of Grater Global Investment, access in July 2011, http://<http://www.iea.org/Papers/2008/chp_report.pdf>.
[7] G. Chicco, P. Mancarella, Trigeneration primary energy saving evaluation for energy planning and policy development, Energy Policy 35 (2007) 6132–6144.
[8] J. Bassols, B. Kuckelkonr, J. Langreck, R. Schneider, H. Veelken, Trigeneration in food industry, Applied Thermal Engineering 22 (2002) 595–602.
[9] R.F. Babus'Haq, J.P. Pearson, S.D. Probert, P.W. O'Callaghan, Economics of mini-combined heat and power packages for use in hotels, Heat Recovery Systems and CHP 10 (1990) 269–275.
[10] A.S. Szklo, J.B. Soares, M.T. Tolmasquim, Energy consumption indicators and CHP technical potential in Brazilian hospital sector, Energy Conversion and Management 45 (2004) 2075–2091.
[11] A. Arteconi, C. Brandoni, F. Polonara, Distributed generation and trigeneration: energy saving opportunities in Italian supermarket sector, Applied Thermal Engineering 29 (2009) 1735–1743.
[12] G.G. Maidment, R.M. Tozer, Combined cooling heat and power in supermarkets, Applied Thermal Engineering 22 (2002) 653–665.
[13] A. Moran, P.J. Mago, L.M. Chamra, Thermoeconomic modeling of micro-CHP (micro-cooling, heating, and power) for small commercial applications, International Journal of Energy Research 32 (2008) 808–823.
[14] E. Cardona, P. Sannino, A. Piacentino, F. Cardona, Energy saving in airports by trigeneration. Part II: short and long term planning for the malpensa 2000 CHCP plant, Applied Thermal Engineering 26 (2006) 1437–1447.
[15] G.G. Maidment, X. Zhao, S.B. Riffat, G. Prosser, Application of combined heat-and-power and absorption cooling in a supermarket, Applied Thermal Engineering 63 (1999) 169–190.
[16] G. Chicco, P. Mancarella, Assessment of greenhouse gas emissions from cogeneration and trigeneration systems. Part I: models and indicators, Energy 33 (2008) 410–417.
[17] B.J.C. Bruno, J. Miquel, F. Castells, Modelling of ammonia absorption chillers integration in energy systems of process plants, Applied Thermal Engineering 19 (1999) 1297–1328.
[18] P. Colonna, S. Gabrielli, Industrial trigeneration using ammonia–water absorption refrigeration systems (AAR), Applied Thermal Engineering 23 (2003) 381–396.
[19] V.H. Gómez, A. Vidal, R. Best, O. García-Valladares, N. Velázquez, Theoretical and experimental evaluation of an indirect-fired GAX cycle cooling system, Applied Thermal Engineering 28 (2008) 975–987.
[20] F.C. Preter, M.S. Rocha, R. Andreos, J.R. Simões-Moreira, Evaluation of a trigeneration system, using microturbine, ammonia–water absorption chiller, and a heat recovery boiler, in: Annals of the 13th Brazilian Congress of Thermal Sciences and Engineering, ABCM, Brazil (2010).
[21] J.C. Ho, K.J. Chua, S.K. Chou, Performance study of a microturbine system for cogeneration application, Renewable Energy 29 (2004) 1121–1133.
[22] X.Q. Kong, R.Z. Wang, J.Y. Wu, X.H. Huang, Y. Huangfu, D.W. Wu, Y.Z. Xu, Experimental investigation of a micro-combined cooling, heating and power system driven by a gas engine, International Journal of Refrigeration 28 (2005) 977–987.
[23] Capstone Turbine Corporation, Microturbine, web site, http://www.capstoneurbine.com, access in July 2011.
[24] Leon Heimer S/A, Internal combustion engines for electrical power production, web site, http://www.heimer.com.br/2009/br/geradores.html, access in July 2011.
[25] CompAir Compressors, Gas compressor, web site, http://www.compaircom, access in July 2011.
[26] Unifin, Heat recovery boiler, web site, http://www.unifin.com, access in July 2011.
[27] Robur Heating Systems, Absorption chillers, web site, http://www.robur.com, access in July 2011.

[28] EPA Regulation 91, Test Methods, Method 02 A, Determination of Gas Velocity and Volumetric Flow Rate in Small Stacks or Ducts Standard Pitot Tube (1982).
[29] EPA Regulation 91, Test Methods, Method 02 C, Direct Measurement of Gas Volume through Pipes and Small Ducts (1982).
[30] EPA Regulation 91, Test Methods, Method 03, Gas Analysis for the Determination of Dry Molecular Weight (1992).
[31] X. Feng, Y. Cai, L. Qian, A new performance criterion for cogeneration systems, Energy Conversion and Management 39 (1998) 1607–1609.
[32] E. Cardona, A. Piacentino, Cogeneration: a regulatory framework toward growth, Energy Policy 33 (2005) 2100–2111.
[33] S. Martínez-Lera, J. Ballester, A novel method for the design of CHCP (combined heat cooling and power) systems for buildings, Energy (2010) 2972–2984.
[34] C.J. Adkins, Equilibrium Thermodynamics, third ed. Cambridge University Press, 1983.
[35] A.S.P. Ortigosa, F.C. Preter, R.L. Labozetto, E.W.Z. Aguilar, J.R. Simões-Moreira, Modeling optimization, and simulation of a commercial ammonia–water absorption refrigeration cycle for production of chilled water, in: Annals of 12th Brazilian Congress of Thermal Engineering and Sciences, ABCM - Brazil (2008).